Phospholipid Bilayer Free Volume Analysis Employing the Thermal Ring-Closing Reaction of Merocyanine Molecular Switches

Christopher J. Wohl,[†] Mandir Ana Helms,[†] Jin O. Chung,[†] and Darius Kuciauskas*[,†,‡]

Department of Chemistry, Virginia Commonwealth University, 1001 West Main Street, Richmond, Virginia 23284-2006, and Department of Chemistry and Biochemistry, Rowan University, 201 Mullica Hill Road, Glassboro, New Jersey 08028

Received: August 21, 2006

The free volume properties of phospholipid bilayers have been determined using a new assay that applies the photochromic and solvatochromic properties of merocyanines. The orientation and embedding depth of the merocyanines in the bilayer are controlled using substitution on the merocyanine indole moiety. The free volume changes at the aqueous interface (region 1), the phospholipid headgroup (region 2), and the aliphatic interior (region 3) of the bilayer are compared by analyzing the rate constants for the merocyanine ring-closing reaction. Free volume variations during the $P_{\beta'}$(gel) ↔ L_{α}(liquid) phase transition are observed in region 1, in accordance with large structural rearrangements between the gel and the liquid phases in this region. The largest free volume is found in region 3, and the smallest is found in region 2. This distribution of free volume in the bilayer agrees with computational studies of these systems. Comparison of the free volume in region 2 of 1,2-dipalmitoyl-*sn*-glycero-3-phosphocholine (DPPC) and 1,2-dimyristoyl-*sn*-glycero-3-phosphocholine (DMPC) lipids shows that this method is sensitive to small structural differences between lipids. In region 2, the free volume is found to be ∼2 times larger in DPPC bilayers, which could be related to different merocyanine interactions with the two phosphatidylcholines. Free volume properties determined on picosecond and second time scales are compared based on an analysis of merocyanine formation and decoloration reactions.

Introduction

Permeability, viscosity, and diffusion in biological membranes depend on the free volume properties of these complex systems. For example, a greater degree of acyl chain unsaturation results in a dramatic increase in the rate of passive trans-bilayer ion flux.[1] This can be directly correlated with an increase in free volume.[2] Simulations have predicted greater bilayer density[3] and reduced free volume[4] as a result of the addition of small amounts of cholesterol to a phospholipid bilayer. Experimentally, this has been observed as reduced diffusion rates of NBD-labeled lipids in phospholipid/cholesterol liposomes.[5] Similarly, the presence of membrane-bound proteins can have a dramatic impact on the distribution of membrane free volume.[6] Embedding of anesthetics into the aqueous interface of phospholipid bilayers is believed to perturb the free volume distribution.[7] This changes the lateral pressure profile, which shifts the ion channel conformation to favor the closed form.[7] Likewise, the incorporation of several small molecules results in dramatic changes in membrane viscosity that may be explained by changes in membrane free volume.[8,9]

In computational studies, a minimum in the free volume was found at the phospholipid headgroups, and a maximum in the ordered aqueous phase and between the lipid leaflets.[2,4,10−12] The current study appears to be the first to experimentally analyze the bilayer free volume profile. We report here the free volume distribution in saturated phosphatidylcholine bilayers using a series of merocyanine/spiropyran molecular sensitizers (Scheme 1) embedded in well-defined regions of the membrane (Scheme 2).

SCHEME 1: Merocyanine and Spiropyran Molecular Sensitizers

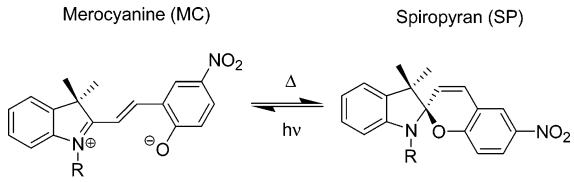

Merocyanines are planar conjugated compounds with a large dipole moment (17.7 D for MC1).[13] The merocyanines shown in Scheme 1 undergo thermal ring-closing reactions described by first-order kinetics.[14] The products of such reactions, spiropyrans, consist of two orthogonal moieties, a substituted indole and benzopyran, connected by a spiro carbon atom. The photochromic and solvatochromic properties of merocyanines have been applied to characterize complex systems, such as glasses.[15−17] The photochemical reactions of membrane-embedded merocyanines, similar to the ones used in this study, have been used to manipulate bilayer permeability to ions and small molecules.[18,19]

Substitution of the indole moiety (R in Scheme 1) was used to control the localization and orientation of merocyanines in the bilayers, which allowed studies of well-defined membrane

* Author to whom correspondence should be addressed. E-mail: kuciauskas@rowan.edu.
[†] Virginia Commonwealth University.
[‡] Rowan University.

10.1021/jp065406y CCC: $33.50
Published on Web 10/25/2006

SCHEME 2: Merocyanine Localization in Different Regions of a Phosphatidylcholine Bilayer and the Structures of DPPC and DMPC Lipids

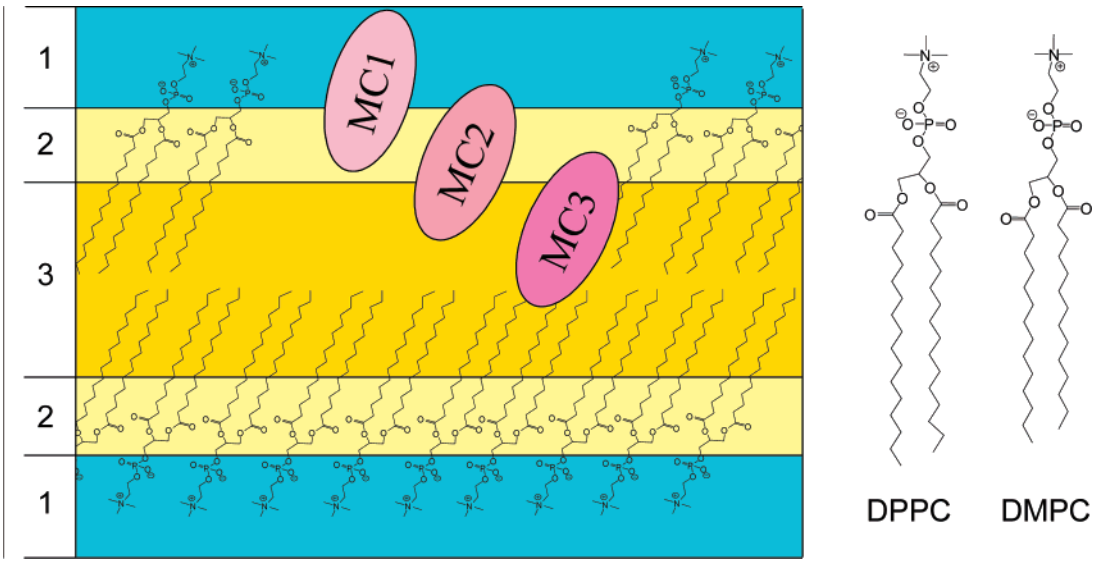

regions. Three-[2,12] and four-region[4,11,20,21] models for the bilayer have been proposed. As illustrated in Scheme 2, MC1 is localized at the surface of the bilayer (region 1, which includes the bilayer/aqueous interface and phosphatidylcholine headgroups), MC2 is found near the phospholipid glycerol backbones and the ordered region of the lipid chains (region 2, which has the highest density), and MC3 is embedded in the aliphatic interior of the bilayer (region 3). We show that the kinetics of the ring-closing reaction for the three merocyanines reflect variations in the phospholipid bilayer free volume.

Experimental Section

Materials and Methods. Deionized water was used in liposome preparation. 1,2-Dimyristoyl-*sn*-glycero-3-phosphocholine (DMPC) and 1,2-dipalmitoyl-*sn*-glycero-3-phosphocholine (DPPC) were obtained from Avanti Polar Lipids. All other reagents, solvents, and 1′,3′-dihydro-1′,3′,3′-trimethyl-6-nitrospiro-[2H-1-benzopyran-2,2′-(2H)-indole] (SP1/MC1) were obtained from Aldrich. (*R*/*S*)-2-(3′,3′-Dimethyl-6-nitro-3′H-spiro[chromene-2,2′-indol]-1′-yl)-ethanol (SP2/MC2) was synthesized using a literature method.[22] (*R*/*S*)-Hexadecanoic acid-2-(3′,3′-dimethyl-6-nitro-3′H-spiro[chromene-2,2′-indol]-1′-yl)-ethyl ester (SP3/MC3) was synthesized as described below. ^{1}H NMR spectra were recorded on a Varian Mercury instrument operating at 299.865 MHz. ^{13}C NMR spectra were recorded on the same instrument operating at 75.400 MHz. Chemical shifts are reported in ppm relative to the residual protonated solvent peak. High-resolution mass spectra were recorded on a Micromass Q-TOF-2 instrument (Manchester, U.K.) using electrospray ionization (positive mode). The samples were introduced into the mass spectrometer using a flow rate of 1 μL/min and a nanospray source, and the needle voltage was set to 2000 V with an ion source at 120 °C and a cone voltage of 35 V. Polyaniline was used for internal calibration. Electronic absorption spectra were measured with a HP8452A diode-array spectrometer and corrected for scattering from the liposomes. Dynamic light scattering measurements were performed with a Zeta Nanosizer ZS (Malvern Instruments).

(*R*/*S*)-Hexadecanoic acid-2-(3′,3′-dimethyl-6-nitro-3′H-spiro[chromene-2,2′-indol]-1′-yl)-ethyl Ester, MC3. (*R*/*S*)-2-(3′,3′-Dimethyl-6-nitro-3′H-spiro[chromene-2,2′-indol]-1′-yl)-ethanol (MC2, 0.71 g, 2.02 mmol) was dissolved in 125 mL of acetonitrile. Pyridine (0.80 g, 10.10 mmol, 5 mol equiv) and palmitoyl chloride (1.67 g, 6.05 mmol, 3 mol equiv) were added to the solution and stirred for 5 h at room temperature until the purple solution became green and a white precipitate formed. The solution was filtered and concentrated under reduced pressure. The crude yellow-brown oil was purified by extraction with ethyl acetate (150 mL) and water (150 mL). The organic layer was washed with water (2 × 150 mL) and dried over $MgSO_4$. The solvent was removed under reduced pressure to afford a crude product as a purple oil (1.80 g). Further purification by column chromatography (silica gel, hexanes/ethyl acetate 4:1) afforded pure **3** (0.66 g, 1.12 mmol) in a 59% yield as a pink solid. ^{1}H NMR (300 MHz, CD_3CN, δ): 8.09 (d, 1H, J = 3 Hz), 8.01 (dd, 1H, J = 9 and 3 Hz), 7.18 (t, 1H, J = 8 Hz), 7.12 (d, 1H, J = 7 Hz), 7.05 (d, 1H, J = 11 Hz), 6.87 (t, 1H, J = 7 Hz), 6.73 (d, 1H, J = 9 Hz), 6.70 (d, 1H, J = 8 Hz), 6.00 (d, 1H, J = 11 Hz), 4.20 (dt, 2H, J = 5 and 3 Hz), 3.55−3.35 (m, 2H), 2.21 (t, 2H, J = 7 Hz), 1.50 (m, 2H), 1.27 (m, 24H), 1.24 (s, 3H), 1.14 (s, 3H), 0.90 (t, 3H, J = 7 Hz). ^{13}C NMR (CD_3CN, δ): 173.7, 159.9, 147.4, 141.7, 136.4, 128.6, 128.2, 126.1, 123.2, 122.4, 122.3, 120.1, 119.5, 115.8, 107.3, 107.2, 62.6, 53.1, 42.7, 34.3, 34.2, 32.2, 29.9−29.2, 25.7, 25.1, 22.9, 19.5, 13.9. MS (ESI, high resolution) $[M + H]^+$ relative intensity 100.00: 591.3773, calcd. for $C_{36}H_{51}N_2O_5$ 591.3798.

Liposome Preparation. Phospholipids and spiropyrans (molar ratio 100:1) dissolved in organic solvents were mixed in a round-bottom flask. The solvent was removed under a N_2 stream. The flask was placed in a warm-water bath (with the temperature above the phospholipid main phase transition), and the phospholipids were hydrated with a phosphate buffer (50 mM, pH 7) to the final phospholipid concentration of 7.4 mM. This aqueous solution was then agitated with a low-power (10 W) ultrasonic bath until homogeneous in appearance and extruded 11 times through a polycarbonate filter (50 nm pore diameter). An average unilamellar vesicle (liposome) diameter of 75 ± 2 nm was determined using dynamic light scattering. Preparation of the supported bilayers used in the linear dichroism experiments is described in the Supporting Information.

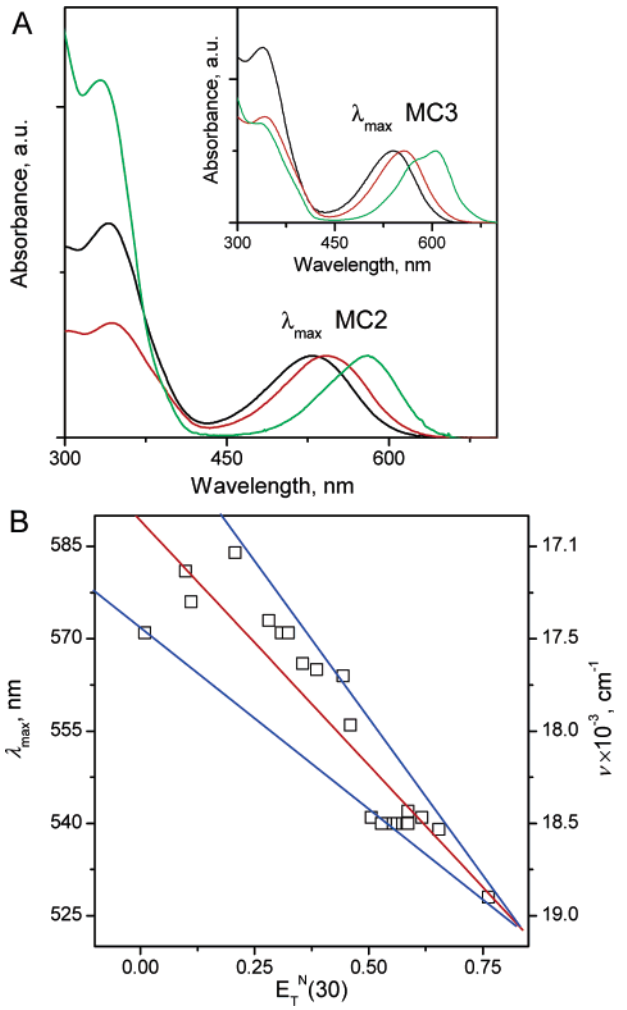

Figure 1. (A) MC2 and MC3 (inset) absorption spectra in methanol (black line, λ_{max} = 528 nm for MC2, 540 nm for MC3), 1-pentanol (red line, λ_{max} = 542 nm for MC2, 555 nm for MC3), and toluene (green line, λ_{max} = 580 nm for MC2, 587 nm for MC3). (B) Solvatochromic shifts for MC2 in organic solvents. Blue lines indicate the maximal deviation of the solvatochromic data from the linear fit.

Kinetics Measurements. Kinetic measurements were conducted using an HP8452A diode-array spectrometer equipped with a temperature-controlled cell holder. For all measurements, the UV (deuterium) lamp of the spectrometer was turned off to prevent merocyanine formation induced by the spectrometer. Samples were placed in 1 cm optical path length quartz cuvettes and were allowed to equilibrate until an external temperature probe displayed a stable temperature for approximately 10 min. The sample cell was exposed to UV illumination (325 nm, Entela hand-held lamp) for 150 s to induce merocyanine formation and allow for equilibration with the bilayer. Sample stability was monitored by measuring its absorption spectrum. Merocyanine aggregation (which could result in absorption band narrowing[23]) was not observed in any of the experiments.

Results

Merocyanine Solvatochromism and Embedding Depth in Phospholipid Bilayers. The electronic absorption spectra of merocyanines MC2 and MC3 in several organic solvents are shown in Figure 1A. The 450−600 nm absorption band is not present for spiropyrans. Therefore, the MC → SP ring-closing kinetics can be studied by following the disappearance of the photochromic absorption band.

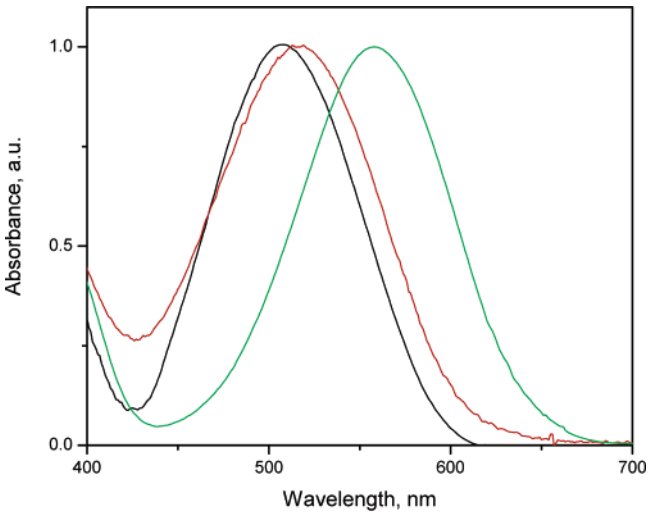

Figure 2. Merocyanine absorption spectra in DPPC bilayers: MC1 (black line, λ_{max} = 505 nm), MC2 (red line, λ_{max} = 520 nm), and MC3 (green line, λ_{max} = 555 nm).

The solvatochromic properties of MC1−MC3 are similar to those of other merocyanines.[24] As shown in Figure 1, the maximum of the photochromic absorption band, λ_{max}, shifts to shorter wavelengths in more polar solvents (for example, λ_{max} for MC2 is at 576 nm in benzene and at 528 nm in ethanol). In agreement with other studies,[25] substitution on the indole moiety does not influence λ_{max} significantly (for example, in toluene solution, λ_{max} = 580 nm for MC1 and MC2 and λ_{max} = 587 nm for MC3). A modified Reichhardt's scale, $E_T^N(30)$, used in the analysis of the solvatochromic shifts in Figure 1B, describes solvent polarity and specific solvent effects, such as hydrogen bonding.[24] An apparent linear correlation between λ_{max} and $E_T^N(30)$ suggests that the polarity of the merocyanine molecular environment can be determined from the maxima of the solvatochromic absorption band.[18,19]

The width of the merocyanine solvatochromic absorption band in phosphatidylcholine bilayers is similar to that in organic solvents (70−80 nm, Figure 2), but λ_{max} shifts from 505 nm for MC1 to 520 nm for MC2 and to 555 nm for MC3. The merocyanine absorption spectra did not change significantly in the 20−60 °C temperature range (Figure S1 in the Supporting Information). As several merocyanine isomers could be present in solution (we have reported the isomeric distribution and excited-state dynamics of MC1),[26] the constant width of the solvatochromic absorption band suggests that the same isomers are present in solvents and bilayers. The most stable MC1−MC3 isomers are shown in Scheme 1.

The solvatochromic shifts in Figure 2 indicate that merocyanines are localized in bilayer regions of different polarities, with $E_T^N(30) \approx 1.12$ for MC1, ~0.97 for MC2, and ~0.42 for MC3. The uncertainty is the largest for MC3, for which $E_T^N(30)$ can range from 0.28 to 0.50 (values typical for cyclohexanone and acetonitrile respectively).[27] Despite this variability, MC3 is in a substantially less polar environment than MC1 or MC2. The polarity variations in the direction of the bilayer normal have been established.[18,19,28] Therefore, merocyanine solvatochromism data indicate that MC1 is localized in region 1, MC2 is found in region 2, and MC3 is embedded deeply into the bilayer (region 3, Scheme 2). Notably, Stern and Feller predicted polarity values at the bilayer/aqueous interface to be higher than the polarity of the bulk water.[28] Our results ($E_T^N(30) > 1$ for MC1, while $E_T^N(30) = 1$ for water) appear to be in agreement with this prediction.

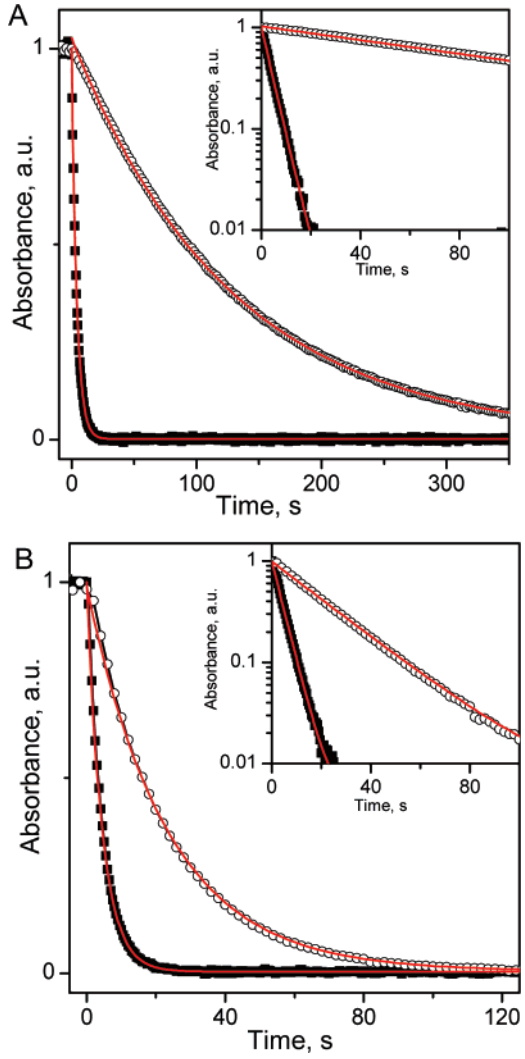

Figure 3. (A) MC1 and (B) MC3 ring-closing kinetics in toluene solution (■) and in L_α phase DPPC bilayers (○) at 50 °C. Insets on the log-linear scale show that the reactions can be described by single-exponential kinetics. Solid lines show single-exponential fits to the data. Rate constants for MC1 are 0.572 ± 0.003 s^{-1} in toluene and (7.86 ± 0.01) × 10^{-3} s^{-1} in bilayers; rate constants for MC3 are 0.584 ± 0.005 s^{-1} in toluene and (4.44 ± 0.01) × 10^{-2} s^{-1} in bilayers.

Merocyanine orientation in phospholipid bilayers was determined from absorption and fluorescence linear dichroism.[29−32] The angle between the bilayer normal and merocyanine transition dipole moment varied from 16° to 45° (Figure S2 in the Supporting Information).

Merocyanine Ring-Closing Kinetics in L_α Phase DPPC Bilayers. Well-defined merocyanine localization in phospholipid bilayers allows characterization of three distinct regions of the membrane from the ring-closing reaction kinetics. Merocyanine reactions were studied in solvent mixtures[33] and in polymers.[15−17] In polymers, however, the kinetics are nonexponential, and more complex models are needed to analyze reaction rates.[15−17] In phospholipid bilayers, single-exponential thermal ring-closing kinetics allow solution-phase models to be used in the analysis.

Merocyanine ring-closing kinetics in DPPC bilayers and in toluene solutions are compared in Figure 3 (temperature T = 50 °C, bilayers are in the liquidlike L_α phase). The kinetics of MC1 and MC3 are similar in toluene solutions (the rate constants are 0.572 ± 0.003 and 0.584 ± 0.005 s^{-1}, respectively). In DPPC bilayers, the ring-closing rate constant decreases ∼70 times for MC1 ((7.86 ± 0.01) × 10^{-3} s^{-1}) and ∼10 times for MC3 ((4.44 ± 0.01) × 10^{-2} s^{-1}). Similar results were obtained for the MC2/DPPC system: The ring-closing rate in the DPPC bilayers is ∼87 times slower than that in toluene solution (respective rate constants are (3.08 ± 0.02) × 10^{-3} and 0.269 ± 0.005 s^{-1})).

In general, the merocyanine ring-closing rates are sensitive to the polarity and viscosity of the reaction medium.[14] The polarity of the aliphatic interior of the bilayer, where MC3 is localized, is similar to that of the toluene solution.[28] Therefore, the slower rate for MC3 in Figure 3B is attributed to the higher viscosity of the DPPC bilayers. For MC1 and MC2, polarity differences could also contribute to the change in rates. We analyzed the temperature dependence of the MC1−MC3 ring-closing reactions to determine the relative contributions of viscosity and polarity effects.

Evidence for the $P_{\beta'} \leftrightarrow L_\alpha$ Phase Transition in the MC1 Rate Constant Data. Figure 4A shows the ring-closing kinetics of MC1/DPPC at several temperatures. All of the kinetics were analyzed as single-exponential decays; the rate constants are summarized in Figure 4B. For comparison, the rate constants determined in toluene solution are also shown. The Arrhenius parameters (the preexponential factor, A, and the activation energy, E_a) were determined by fitting the rate constant temperature dependence data to the expression

$$k = A \exp(-E_a/RT) \quad (1)$$

where R is the gas constant. E_a = 71 ± 1 kJ mol^{-1} determined in toluene solution (Figure 4B and Table 1) is in excellent agreement with the literature value of 70.1 kJ mol^{-1}.[33,34]

For the MC1/DPPC system, the slope of the Arrhenius graph decreases from E_a = 191 ± 22 kJ mol^{-1} at <40 °C to E_a = 81 ± 9 kJ mol^{-1} at >40 °C. For MC1/DMPC, E_a decreases from 128 ± 25 kJ mol^{-1} at <23 °C to 78 ± 3 kJ mol^{-1} at >23 °C (Table 1). This change in activation energy can be attributed to the gel−liquid ($P_{\beta'} \leftrightarrow L_\alpha$) phase transition, which occurs at ∼41 °C for DPPC and ∼23 °C for DMPC bilayers.[35] During the $P_{\beta'} \leftrightarrow L_\alpha$ phase transition, the structure of the bilayer changes from the more ordered $P_{\beta'}$ gel phase to the liquidlike L_α phase. The changes in the bilayer structure are the most significant in the phospholipid headgroup region and at the aqueous interface (region 1).[35] As MC1 is found at the interface, ring-closing kinetics reflect bilayer structural rearrangements due to the $P_{\beta'} \leftrightarrow L_\alpha$ phase transition. Activation energies in both phases of the bilayer are higher than E_a = 71 kJ mol^{-1} in toluene solution, which is attributed to the higher viscosity and polarity of bilayer region 1 relative to toluene.

MC2 and MC3 Kinetics in DMPC and DPPC Bilayers. The temperature dependence of the ring-closing rate constants for MC2 and MC3 in bilayers and in toluene are shown in Figure 5; the Arrhenius parameters are summarized in Table 1.

The MC3 kinetics in DMPC and DPPC bilayers are the same, within experimental uncertainty. This suggests that the molecular environment surrounding this merocyanine is similar in both bilayers. The results for MC2 are different—the rate constants for MC2/DPPC are ∼100 times lower than those for MC2/DMPC. (In addition, for MC2/DMPC, E_a is higher by ∼30% in the L_α phase, while no such change is evident for MC2/DPPC.) The contrasting data for MC2/DPPC and MC2/DMPC suggests that either the free volume of the glycerol backbone region of these two lipids is not identical (see Discussion) or MC2 perturbs the local structure of the bilayer differently for these two phosphatidylcholines. As DPPC and DMPC lipids have identical headgroups and only differ in the lengths of their acyl chains (Scheme 2), this sensitivity is surprising. The

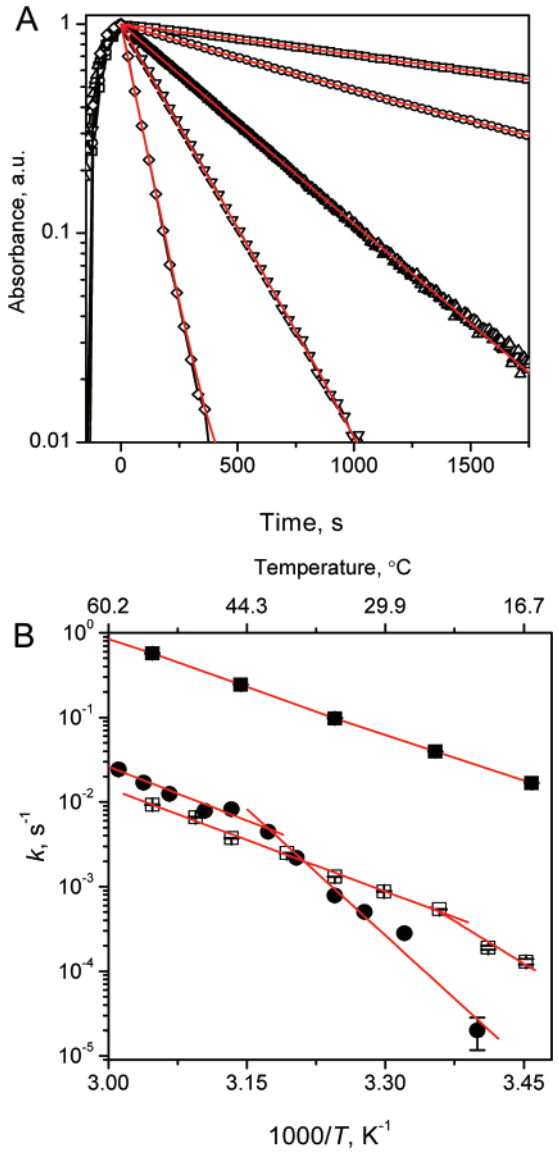

Figure 4. (A) MC1/DPPC ring-closing kinetics at 28 °C (□, (2.80 ± 0.09) × 10^{-4} s^{-1}), 35 °C (○, (7.90 ± 0.01) × 10^{-4} s^{-1}), 39 °C (△, (2.20 ± 0.01) × 10^{-3} s^{-1}), 42 °C (▽, (4.47 ± 0.02) × 10^{-3} s^{-1}), and 53 °C (◇, (1.25 ± 0.01) × 10^{-2} s^{-1}). Single-exponential fits are shown as solid lines. (B) Temperature dependence of the MC1 ring-closing rate constant, *k*, in DPPC (●) and DMPC (□) bilayers and in toluene solution (■). Solid lines are fits according to the Arrhenius expression. The change in activation energy for MC1/DMPC (at ~23 °C) and MC1/DPPC (at ~40 °C) is attributed to the $P_{\beta'} \leftrightarrow L_\alpha$ phase transition.

isomerizing molecular probes could be more sensitive to the bilayer structural variations in this region, because the molecular density is the highest in the glycerol backbone region (and the free volume is the smallest).[21]

Discussion

In the Results section, we showed that merocyanine ring-closing kinetics, rate constants, and Arrhenius parameters that describe the rate constant temperature dependence vary (i) in regions 1−3 of the bilayer (Scheme 2) and (ii) for phosphatidylcholines with different saturated acyl chain lengths. Now we apply models from condensed-phase reaction dynamics[36] to analyze the free volume properties of these bilayer systems.

Rate Constant Analysis Using a Kramers' Model. Effects from the molecular activation energy, E_0, and the viscosity, η, on the rate constants can be determined from[36]

$$k \propto \frac{1}{\eta^a} \exp\left[-\frac{E_0}{RT}\right] \quad (2)$$

Classical Kramers' theory predicts that the exponent *a* is equal to 1 ($a = 1$).[36] When the Kramers' model was applied to protein folding,[37] ring-closing reactions,[38] and isomerization of cyanine dyes,[39−41] it was found that in systems with relatively high viscosities the power law dependence predicted by classical Kramers' theory fails, but $a < 1$ could adequately explain the data.[36,42]

The temperature dependence for the viscosity, η, is commonly written as[43]

$$\eta(T) = \eta_0 \, e^{(E_\eta/RT)} \quad (3)$$

where η_0 is the viscosity as temperature approaches infinity and E_η is the viscosity activation energy. Dipyrenylpropane excimer studies yielded $E_\eta = 35$ kJ mol^{-1} for L_α phase phosphatidylcholines.[44,45] In more recent triplet radical ion pair recombination studies, it was found that $E_\eta = 35.6$ kJ mol^{-1} in the lipid headgroup region but $E_\eta = 73.6$ kJ mol^{-1} in the aliphatic interior of the bilayer.[43] Therefore, we assumed that $E_\eta = 35.6$ kJ mol^{-1} in regions 1 and 2 of the bilayer[43−45] and that $E_\eta = 73.6$ kJ mol^{-1} in region 3.[43] (Our analysis is limited to L_α phase bilayers, as the viscosity and viscosity activation energy in the $P_{\beta'}$ phase are not established.)

Comparison of eqs 1−3 shows that the Arrhenius activation energy is related to the molecular activation energy, E_0, and the viscosity activation energy, E_η[17]

$$E_a = E_0 + aE_\eta \quad (4)$$

To estimate aE_η, the E_0 should be determined independently.[36] In the temperature range used in our studies, the viscosity of toluene varies much less than the viscosity of the bilayer (viscosity activation energy for toluene $E_{\eta,\text{toluene}} = 9.2$ kJ mol^{-1}).[46] Therefore, we estimated molecular activation energies as $E_0 = E_{a,\text{toluene}} - E_{\eta,\text{toluene}}$ and assumed that the *a* value in toluene is unity. Such analysis yields E_0 values in close agreement with the results for merocyanines derived from spirooxazines.[17] Results of the free volume analysis for MC1−MC3 reactions in DMPC and DPPC bilayers are summarized in Table 2.

Phosphatidylcholine Bilayer Free Volume. The exponent *a* in Table 2 is proportional to the available free volume, V_f[39,47]

$$a \propto \frac{V_f}{V_0} \quad (5)$$

where V_0 is the molecular volume required for the reaction. Through the use of laser-induced optoacoustic spectroscopy, the volume change due to the MC1 photochemical reaction was determined to be ~78 $Å^3$ $molecule^{-1}$ (in cycloalkane solvents).[48] Therefore, merocyanine photochromic molecular switches could detect free volume changes of a similar magnitude.

Phosphatidylcholine bilayer free volume has been investigated in computational studies.[2,4,10−12,21] The total free volume in the bilayer midplane has been calculated to be as large as 54% for a DPPC membrane;[6] however, V_f is less than the total free volume. The available free volume depends on the size of the solute and on the distribution of the free volume "voids" in the bilayers. Free volume voids have been predicted to be larger in the bilayer midplane than in the ordered aqueous phase.[11] These voids often have the shape of elongated ellipsoids.[12] The highest density (and smallest V_f) is found in region 2.[21] Because of the

TABLE 1: Merocyanine MC1−MC3 Photophysical Properties in Toluene Solution and in Phosphatidylcholine Bilayers

		E_a (kJ mol^{-1}), ln(A)				
		DMPC bilayer[b]		DPPC bilayer[c]		
	λ_{max}[a] (nm)	L_α	$P_{\beta'}$	L_α	$P_{\beta'}$	toluene
MC1	501−507	78 ± 3, 23.8 ± 1.1	128 ± 25, 44.0 ± 10.2	81 ± 9, 25.7 ± 3.3	191 ± 22, 67.4 ± 8.7	71 ± 1, 25.5 ± 0.1
MC2	512−520	85 ± 5, 29.4 ± 0.6	63 ± 2, 20.6 ± 0.4	100 ± 3, 31.7 ± 1.0		77 ± 4, 27.7 ± 1.7 [d]
MC3	549−555	124 ± 3, 43.4 ± 1.1		123 ± 6, 43.1 ± 2.5		76 ± 1, 27.4 ± 0.1

[a] Maximum of the solvatochromic and photochromic merocyanine absorption band in DMPC and DPPC bilayers determined over the temperature range 20−60 °C. [b] $P_{\beta'} \leftrightarrow L_\alpha$ phase transition temperature ~23 °C. [c] $P_{\beta'} \leftrightarrow L_\alpha$ phase transition temperature ~41 °C. [d] MC2 kinetics in toluene were biexponential. The amplitude of the second component was <30% of the total amplitude, the lifetime was ~10 times longer than that of the first, and the activation energy was 25 ± 9 kJ mol^{-1}.

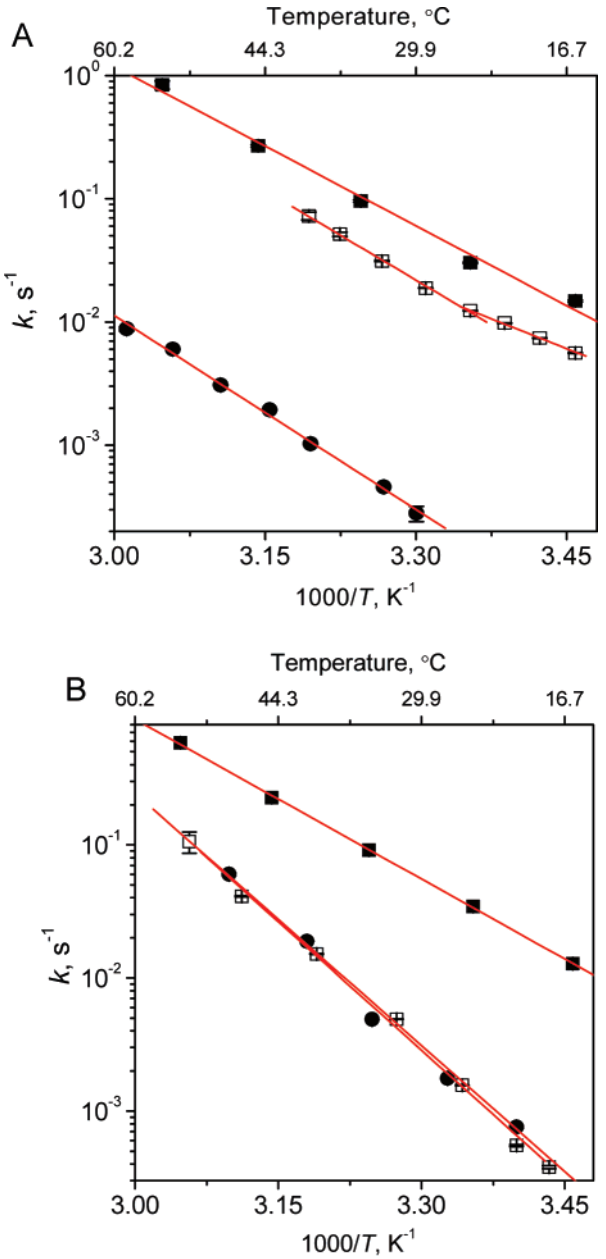

Figure 5. (A) MC2 and (B) MC3 ring-closing rate constant temperature dependence in DPPC (●) and DMPC (□) bilayers and in toluene solution (■). Solid lines are fits according to the Arrhenius expression.

uncertainty in estimating V_0 for merocyanines and spiropyrans, we cannot determine absolute V_f values. Rather, we analyze V_f variation in the direction of the bilayer normal.

For MC3 (region 3 in Scheme 2), exponent a values in DPPC and DMPC bilayers are identical, $a = 0.76-0.77$. Thus, the aliphatic region of the bilayer is similar for both phosphatidylcholines. In addition, the same Arrhenius activation energy describes the temperature dependence of rate constants in the L_α and $P_{\beta'}$ phases. This result is in agreement with smaller structural changes in this region of the bilayer during the liquid−gel phase transition.

For MC1 (region 1), $a = 0.45$ for DMPC bilayers, and $a = 0.53$ for DPPC bilayers. This result suggests that V_f is somewhat lower in the L_α phase of the DMPC bilayers; however, the difference is not large relative to the uncertainty of the data. As shown in Figure 4B and Table 1, MC1 ring-closing rate constants in DPPC and DMPC bilayers differ more significantly in the $P_{\beta'}$ phase. This result might be related to the different orientation of MC1 in the gel phase of these bilayers. (The angle between the bilayer normal and the merocyanine dipole moment was 16° in DPPC bilayers and 25° in DMPC bilayers; see Figure S2 in the Supporting Information.)

The most interesting results are obtained from the MC2 data. This merocyanine is localized in region 2, which includes the glycerol backbone and the ordered region of the acyl chains. As shown in Figure 5A, the rate constants for MC2 in the DPPC and DMPC bilayers differ by almost 2 orders of magnitude, and the available free volume exponents are $a = 0.90$ for DPPC and $a = 0.48$ for DMPC (Table 2). This suggests that in region 2 the available free volume is approximately 2 times larger in the DPPC bilayers. This outcome could reflect intrinsic properties of the bilayers or could be induced by the membrane-embedded merocyanines.

In computational studies, the free volume properties of DMPC and DPPC bilayers were found to be very similar in all membrane regions.[21] Thus, our results agree with computational free volume analyses for regions 1 and 3 but not for region 2. This region of the membrane is the most densely packed. (The total free volume is ~30% less than that in region 3 and ~15% less than that in region 1.[11]) When the available free volume is considered, the differences between the bilayer regions are even more pronounced.[11] If merocyanines are perturbing the local structure of the bilayer, then such perturbations are likely to have the largest effect in the most dense membrane region. The presence of cholesterol (mole fraction of 0.4) in DMPC bilayers led to a reduction in the free volume in the bilayer midplane and an increase in free volume in the headgroup region.[12]

In experimental studies, differences between DMPC and DPPC bilayers have been reported. For example, the antimicrobial peptide microcin J25 was shown to induce a dramatic fluidity change in DPPC membranes but not in DMPC membranes.[49] The membrane microviscosity variation demonstrated by this peptide may be related to the available free volume.

We found that the largest available free volume is in region 3, and the smallest at the interface (region 1). For DMPC bilayers, the largest change in V_f (more than 150% increase)

TABLE 2: Analysis of the Free Volume Properties of L_α Phase Phosphatidylcholine Bilayers

	E_a (kJ mol^{-1})			aE_η (kJ mol^{-1})		free volume exponent a	
	DMPC	DPPC	E_0 (kJ mol^{-1})	DMPC	DPPC	DMPC	DPPC
MC1	78 ± 3	81 ± 9	62 ± 1	16.0 ± 0.3	19.0 ± 1.1	0.45 ± 0.03[a]	0.53 ± 0.05[a]
MC2	85 ± 5	100 ± 3	68 ± 4	17.0 ± 0.6	32.0 ± 1.4	0.48 ± 0.04[a]	0.90 ± 0.07[a]
MC3	124 ± 3	123 ± 6	67 ± 1	57.0 ± 1.3	56.0 ± 2.4	0.77 ± 0.06[b]	0.76 ± 0.09[b]

[a] $E_\eta = 35.6$ kJ mol^{-1} was assumed.[43−45] [b] $E_\eta = 73.6$ kJ mol^{-1} was assumed.[43]

takes place between regions 2 and 3. For DPPC bilayers, a similar increase in V_f is observed between the regions 1 and 2.

Phospholipid Bilayer Dynamics and Free Volume. Phospholipid dynamics range from picoseconds (trans/gauche isomerizations) to hours (lipid exchange between the bilayer leaflets),[50] and therefore the bilayer free volume will depend on the time scale of the reaction that is used to probe this complex system. SP → MC and MC → SP reaction dynamics are uniquely suitable for such an analysis as the ultrafast ring-opening reaction, SP → MC, occurs on the picosecond time scale, while the thermal ring-closing reaction, MC → SP, is much slower. On the picosecond time scale, major bilayer reorganizational dynamics are essentially "frozen", and ultrafast reactions reveal the static structure of the bilayer. On the slower time scale studied in this work, the phospholipids can rearrange in response to the photochemical reaction.

Recently we studied the ultrafast ring opening and isomerization of spiropyran SP2 (SP2 → MC2) in the aliphatic region 3 of DPPC, DMPC, and 1,2-di-oleoyl-*sn*-glycero-3-phosphocholine (DOPC) bilayers.[51] On the picosecond time scale in L_α phase bilayers, the free volume exponent was $a = 0.33 \pm 0.03$, much smaller than $a = 0.76-0.77$ determined in the current study for region 3. The difference suggests that on a picosecond time scale V_f is approximately 2 times smaller than on the time scale examined here.

Comparison of data measured at different time scales shows other differences. For the slower reactions studied here, E_a was generally higher in the $P_{\beta'}$ phase than that in the L_α phase (Table 1), which is consistent with the presumed higher viscosity of the gel phase bilayers. In contrast, on the picosecond time scale, E_a in region 3 increased from 7.3 kJ mol^{-1} in the $P_{\beta'}$ phase to 26 kJ mol^{-1} in the L_α phase.[51] Although this hypothesis requires further study, the smaller E_a values for ultrafast reactions in $P_{\beta'}$ phase could be related to the free volume void aggregation around spiropyrans in the bilayer, similar to the cholesterol effects found in simulations.[4]

The time scale of many biological processes, such as diffusion in the membrane or transport across the bilayer, occurs on a millisecond and second time scale. Thus, the results of the current experiments could be more directly applicable to biological membrane phenomena than the results of ultrafast studies[51] and picosecond time scale simulations.[2,4,11,12,20,21]

Conclusions

Photochromic and solvatochromic merocyanines appear to be sensitive molecular probes of phospholipid bilayer structure and dynamics: (i) Merocyanines can be embedded into well-defined regions of the bilayer, (ii) ring-closing rate constants are sensitive probes of the structural changes that occur during gel−liquid phase transitions, (iii) even small differences in bilayer properties (such as the contrasting free volume properties in region 2 of DMPC and DPPC bilayers) are reflected in the rate constant data, and (iv) bilayer properties on ultrafast (picosecond) and slow (second) time scales can be analyzed using merocyanine and spiropyran reactions.

We determined the free volume profile of saturated phosphatidylcholine bilayers and developed a new method to study this important physical property. This method, based on the rate constant analysis of intramolecular ring-closing reactions, can be applied to other bilayer systems. Computational studies showed that alkyl chain unsaturation[2] and gauche conformations[52] result in enhanced free volume, while branching in the alkyl chains[53] and the presence of cholesterol[4] reduce the available free volume. These predictions remain to be tested experimentally. Our method could also be applied to the analysis of the free volume distribution in bilayers with components segregated into domains. The results described in this paper suggest that molecular probes in region 2 of the bilayer are the most sensitive to the variation of membrane properties and could be applied to analyze lipid self-segregation behavior. To study bilayer domains, photochemical molecular probes with affinities to these membrane regions should be developed. Such studies are in progress.

Acknowledgment. We thank the Jeffress Memorial Trust and Virginia Commonwealth University for support.

Supporting Information Available: Merocyanine absorption spectra in the gel and liquid phases of the bilayer and merocyanine orientational distribution functions determined using supported bilayers. This material is available free of charge via the Internet at http://pubs.acs.org.

References and Notes

(1) Zeng, Y.; Han, X.; Gross, R. W. *Biochemistry* **1998**, *37*, 2346.
(2) Rabinovich, A. L.; Balabaev, N. K.; Alinchenko, M. G.; Voloshin, V. P.; Medvedev, N. N.; Jedlovszky, P. *J. Chem. Phys.* **2005**, *122*, 084906.
(3) Jedlovszky, P.; Mezei, M. *J. Phys. Chem. B* **2003**, *107*, 5311.
(4) Falck, E.; Patra, M.; Karttunen, M.; Hyvonen, M. T.; Vattulainen, I. *J. Chem. Phys.* **2004**, *121*, 12676.
(5) Almeida, P. F. F.; Vaz, W. L. C.; Thompson, T. E. *Biochemistry* **1992**, *31*, 7198.
(6) Bachar, M.; Becker, O. M. *Biophys. J.* **2000**, *78*, 1359.
(7) Cantor, R. S. *Biochemistry* **1997**, *36*, 2339.
(8) Ferreira, H.; Lucio, M.; Lima, J. L. F. C.; Cordeiro-da-Silva, A.; Tavares, J.; Reis, S. *Anal. Biochem.* **2005**, *339*, 144.
(9) Bahri, M. A.; Heyne, B. J.; Hans, P.; Seret, A. E.; Mouithys-Mickalad, A. A.; Hoebeke, M. D. *Biophys. Chem.* **2005**, *114*, 53.
(10) Shinoda, W.; Mikami, M.; Baba, T.; Hato, M. *J. Phys. Chem. B* **2003**, *107*, 14030.
(11) Marrink, S. J.; Sok, S. M.; Berendsen, H. J. C. *J. Chem. Phys.* **1996**, *104*, 9090.
(12) Alinchenko, M. G.; Voloshin, V. P.; Medvedev, N. N.; Mezei, M.; Partay, L.; Jedlovszky, P. *J. Phys. Chem. B* **2005**, *109*, 16490.
(13) Bletz, M.; Pfeifer-Fukumura, U.; Kolb, U.; Baumann, W. *J. Phys. Chem. A* **2002**, *106*, 2232.
(14) Horie, K.; Ushiki, H.; Winnink, F. M. *Molecular Photonics: Fundamentals and Practical Aspects*; Wiley-VCH: Weinheim, Germany, 2000.
(15) Richert, R.; Heuer, A. *Macromolecules* **1997**, *30*, 4038.
(16) Levitus, M.; Talhavini, M.; Negri, R. M.; Atvars, T. D. Z.; Aramendia, P. F. *J. Phys. Chem. B* **1997**, *101*, 7680.
(17) Volker, E.; O'Connell, M.; Negri, R. M.; Aramendia, P. F. *Helv. Chim. Acta* **2001**, *84*, 2751.
(18) Khairutdinov, R. F.; Hurst, J. K. *Langmuir* **2001**, *17*, 6881.
(19) Khairutdinov, R. F.; Hurst, J. K. *Langmuir* **2004**, *20*, 1781.
(20) Marrink, S.-J.; Berendsen, H. J. C. *J. Phys. Chem.* **1994**, *98*, 4155.

(21) Kupiainen, M.; Falck, E.; Ollila, S.; Niemela, P.; Gurtovenko, A. A.; Hyvonen, M. T.; Patra, M.; Karttunen, M.; Vattulainen, I. *J. Comput. Theor. Nanosci.* **2005**, *2*, 401.
(22) Raymo, F. M.; Giordani, S.; White, A. J. P.; Williams, D. J. *J. Org. Chem.* **2003**, *68*, 4158.
(23) Seki, T.; Ichimura, K. *J. Phys. Chem.* **1990**, *94*, 3769.
(24) Rosario, R.; Gust, D.; Hayes, M.; Springer, J.; Garcia, A. A. *Langmuir* **2003**, *19*, 8801.
(25) Wojtyk, J. T. C.; Wasey, A.; Kazmaier, P. M.; Hoz, S.; Buncel, E. *J. Phys. Chem. A* **2000**, *104*, 9046.
(26) Wohl, C. J.; Kuciauskas, D. *J. Phys. Chem. B* **2005**, *109*, 22186.
(27) Reichardt, C. *Chem. Rev.* **1994**, *94*, 2319.
(28) Stern, H. A.; Feller, S. E. *J. Chem. Phys.* **2003**, *118*, 3401.
(29) Castanho, M.; Lopes, S.; Fernandes, M. *Spectrosc.: Int. J.* **2003**, *17*, 377.
(30) Lopes, S.; Fernandes, M. X.; Prieto, M.; Castanho, M. A. R. B. *J. Phys. Chem. B* **2001**, *105*, 562.
(31) Lopes, S. C. D. N.; Goormaghtigh, E.; Cabral, B. J. C.; Castanho, M. A. R. B. *J. Am. Chem. Soc.* **2004**, *126*, 5396.
(32) Lopes, S.; Castanho, M. A. R. B. *J. Phys. Chem. B* **2002**, *106*, 7278.
(33) Sciaini, G.; Wetzler, D. E.; Alvarez, J.; Fernandez-Prini, R.; Laura Japas, M. *J. Photochem. Photobiol., A* **2002**, *153*, 25.
(34) Wetzler, D. E.; Aramendia, P. F.; Japas, M. L.; Fernandez-Prini, R. *Phys. Chem. Chem. Phys.* **1999**, *1*, 4955.
(35) *The Structure of Biological Membranes*; CRC Press: Boca Raton, FL, 1992.
(36) Waldeck, D. H. The role of solute−solvent friction in large amplitude motions. In *Conformational Analysis of Molecules in Excited States*; Waluck, J., Ed.; Wiley-VCH: New York, 2000; p 113.
(37) Jas, G. S.; Eaton, W. A.; Hofrichter, J. *J. Phys. Chem. B* **2001**, *105*, 261.
(38) Lipson, M.; Peters, K. S. *J. Phys. Chem. A* **1998**, *102*, 1691.
(39) Aakesson, E.; Hakkarainen, A.; Laitinen, E.; Helenius, V.; Gillbro, T.; Korppi-Tommola, J.; Sundstroem, V. *J. Chem. Phys.* **1991**, *95*, 6508.
(40) Aramendia, P. F.; Negri, R. M.; Roman, E. S. *J. Phys. Chem.* **1994**, *98*, 3165.
(41) Onganer, Y.; Yin, M.; Bessire, D. R.; Quitevis, E. L. *J. Phys. Chem.* **1993**, *97*, 2344.
(42) Murarka, R. K.; Bhattacharyya, S.; Biswas, R.; Bagchi, B. *J. Chem. Phys.* **1999**, *110*, 7365.
(43) Shafirovich, V. Y.; Batova, E. E.; Levin, P. P. *J. Am. Chem. Soc.* **1995**, *117*, 6093.
(44) Turley, W. D.; Offen, H. W. *J. Phys. Chem.* **1986**, *90*, 1967.
(45) Zachariasse, K. A.; Kuenle, W.; Weller, A. *Chem. Phys. Lett.* **1980**, *73*, 6.
(46) Harris, K. *J. Chem. Eng. Data* **2000**, *45*, 893.
(47) Gegiou, D.; Muszkat, K. A.; Fischer, E. *J. Am. Chem. Soc.* **1968**, *90*, 3907.
(48) Williams, R. M.; Klihm, G.; Braslavsky, S. E. *Helv. Chim. Acta* **2001**, *84*, 2557.
(49) Rintoul, M. R.; de Arcuri, B. F.; Morero, R. D. *Biochim. Biophys. Acta* **2000**, *1509*, 65.
(50) Laggner, P.; Kriechbaum, M. *Chem. Phys. Lipids* **1991**, *57*, 121.
(51) Wohl, C. J.; Kuciauskas, D. *J. Phys. Chem. B* **2005**, *109*, 21893.
(52) Pradhan, G. R.; Pandit, S. A.; Gangal, A. D.; Sitaramam, V. *J. Theor. Biol.* **2003**, *220*, 189.
(53) Shinoda, W.; Mikami, M.; Baba, T.; Hato, M. *Chem. Phys. Lett.* **2004**, *390*, 35.